Can hydrocarbons in coastal sediments be related to terrestrial flux? A case study of Godavari river discharge (Bay of Bengal)

Rayaprolu Kiran[1], V. V. J. Gopala Krishna[1], B. G. Naik[1], G. Mahalakshmi[2], R. Rengarajan[3], Aninda Mazumdar[2] and Nittala S. Sarma[1,*]

[1]Marine Chemistry Laboratory, Andhra University, Visakhapatnam 530 003, India
[2]National Institute of Oceanography, Dona Paula, Goa 403 004, India
[3]Physical Research Laboratory, Navrangpura, Ahmedabad 380 009, India

A sediment core aged ~250 years and deposition rate of ~2.4 mm yr^{-1} raised from the coastal region receiving inputs from the Godavari river was examined for *n*-alkanes. The carbon preference index (CPI) of short-chain hydrocarbons (SHC) indicated intense bacterial activity. The long-chain hydrocarbons (LHC) were major and their CPI (CPI$_{LHC}$) indicated that the terrestrial source was more dominant compared to the *in situ* input. CPI$_{LHC}$ is significantly linearly correlated and appears to be a proxy for the historical discharge of the river.

Keywords: Carbon preference index, coastal sediments, hydrocarbons, terrestrial flux.

ORGANIC matter (OM) in coastal sediments is derived from various sources such as terrigenous, marine, atmospheric and anthropogenic[1,2]. Lipids account for a small fraction of OM. When characterized at the molecular level, they can provide valuable information on the sources, e.g. allochthonous, autochthonous, biogenic, petrogenic, etc.[3]. The lipid molecules particularly useful for source characterization are *n*-alkanes, fatty acids, alcohols and sterols[4,5]. *n*-Alkanes are one of the most stable group of compounds retaining their original structure during sediment diagenesis. Also, the ease of analysis and availability of hydrocarbon standards commercially, make hydrocarbons one of the most frequently investigated class of compounds in organic geochemistry[6].

The western Bay of Bengal, along the east coast of the Indian peninsular region, is an area extensively influenced by inputs from rivers, in particular by Cauvery, Krishna, Godavari and Mahanadi. The silt delivered by these rivers during floods is advectively transported away from the river mouths by coastal currents. The finer fraction of suspended particles from River Godavari are transported northwards and deposited as clayey silt or mixed sediment (sand–silt–clay) up to Kalingapatnam[7]. Water column primary production of the coastal region away from the river mouth quickly falls northwards. Due

to these two factors, the sediment deposits in the near-shore region of the western Bay of Bengal, essentially reflect the fluvial discharge and its particulates. To our knowledge, sediment biomarkers have not been investigated to establish a possible link with the historical record of terrestrial discharge rates. The objective of this communication is to explore a potential quantitative link between the sediment-preserved hydrocarbons and discharge by the River Godavari.

All chemicals used were of analytical grade. The solvents were of HPLC grade and were double-distilled before use.

Three sediment cores were raised using a gravity corer on-board *CRV Sagar Purvi* from the silt zone of the near-shore seafloor occurring at 30–50 m column depth between Pentakota and Kalingapatnam. The 65 cm long core raised off Pentakota (30 m; 17°12′42″N, 82°40′36″E) was the only undisturbed core as revealed by ^{210}Pb dating. The core was sliced at intervals of 1 cm up to 10 cm from the top, 2 cm in the 10–20 cm section and 3 cm further down. The sediment fractions were split into two halves. One half was frozen dry and thrashed with nickel spatula to fine dry powder. The other half of the sediment fractions was oven-dried (at 60°C for 12–24 h until constant weight was obtained) and the powders were subjected to ^{210}Pb dating, and organic carbon (C_{org}) estimation. C_{org} was determined using the wet digestion method[8].

Lead isotopic dating was performed at the Physical Research Laboratory, Ahmedabad. The ^{210}Pb, ^{137}Cs and ^{226}Ra isotope concentrations were determined by non-destructive gamma counting[9,10]. Approximately 4 g (mean ± SD, 3.8 ± 0.7 g) of the dried and powdered sediment sample was packed in a plastic vial, sealed and placed in a high purity germanium (HPGE) coaxial 16 × 40 mm well-type detector (Canberra Industries, CT, USA) after the *γ*-emitting daughter products of ^{210}Pb reached secular equilibrium with it in approximately 3 weeks. The system was calibrated with U–Th standards as well as those of ^{210}Pb and ^{137}Cs. The ^{210}Pb standards were also prepared the same way as the samples. In general, each sample was counted for approximately 3 days. The core was shown to be undisturbed with an age of 252.3 years. The sedimentation rate was calculated assuming it to be uniform at 2.537 mm yr^{-1} ($n = 4$, $R^2 = 0.97$).

The freeze-dried sediment sample (15 g) was taken in an extraction thimble and placed in a Soxhlett apparatus and extracted with hot $CH_3OH : CH_2Cl_2$ mixture (1 : 1) for 12 h, by which time the extraction was complete (~100 cycles; close to 100% recovery of an externally added standard hexatriacontane (Sigma), a C_{36} saturated hydrocarbon). The clear extract was decanted into a beaker containing copper turnings (5 g) and the contents were sonicated at room temperature (RT) for 1 h to remove any elemental sulphur that might be present[11]. The filtrate passing through Whatman filter paper no. 42 was saponified (using KOH : MeOH-MilliQ H_2O, 90 : 10, 7 ml, RT, overnight). The contents were diluted with 2 ml
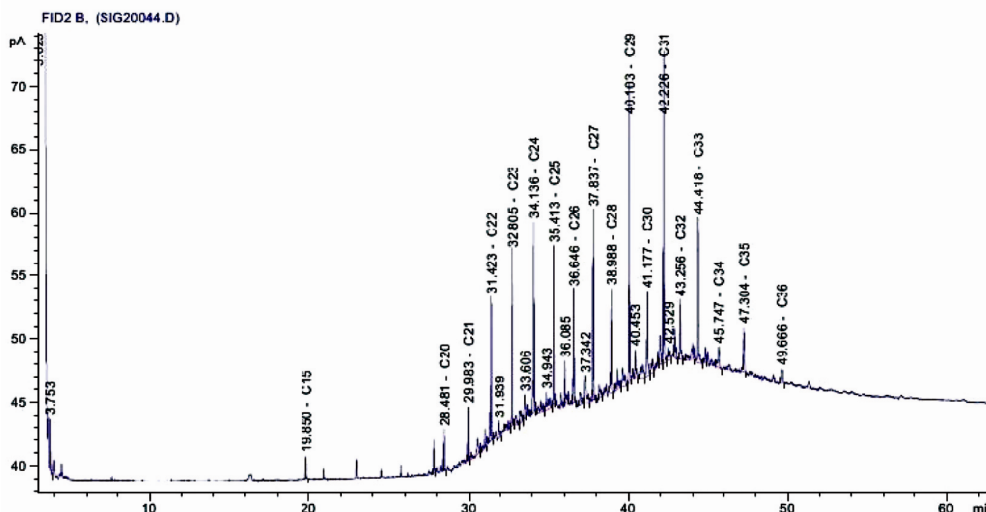
*For correspondence. (e-mail: nssarma@rediffmail.com)

Figure 1. Typical gas chromatogram of hydrocarbon fraction (of the 9 cm section, i.e. 36 yrs BP).

MilliQ H_2O, and extracted repeatedly with small volumes of hexane containing diethyl ether (9 : 1). The organic layer at the top was pooled, washed twice with cold MilliQ water, dried over anhydrous Na_2SO_4 and the residue of non-acidic lipids was obtained in the rotavapor. The aqueous layer was not pursued.

The residue from the above procedure was separated into three fractions by column chromatography (1 × 30 cm) over a bed of silica gel, deactivated (with MilliQ water, 5%) and set in *n*-hexane. Successive elution with 40 ml each of hexane, hexane : toluene (4 : 1) and hexane : ethyl acetate (4 : 1) followed by evaporation of the fractions left residues that were quantitatively transferred, the solvent evaporated and redissolved in a constant volume of *n*-hexane (200 μl) for gas chromatographic analysis.

Gas chromatography–mass chromatographic (GC–MS) analyses were performed using a Shimadzu QP-2010 Gas Chromatograph and Mass Spectrometer interfaced with AOC-20i auto sampler with fused silica capillary column RXi-5 (RESTEK, 30 m × 0.25 mm id × 0.25 μm film thickness), at the National Institute of Oceanography, Goa. Helium was used as carrier gas. The injector and detector temperatures were set to 280°C and 320°C respectively. The oven temperature programme was: 40°C (1 min), 40–140°C @ 10°C min^{-1}, 140–320°C @ 6°C min^{-1}, 320°C (15 min). The hydrocarbons identified were the normal C_8–C_{38} saturated hydrocarbons of biogenic origin.

The sediment was clayey silt throughout and no $CaCO_3$ shells were found in the freeze dried powders. C_{org} was low (0.39–0.72%, mean ± SD, 0.5 ± 0.08%). The total hydrocarbon concentration (THC) ranged from 0.014 to 0.704 ppm. In the gas chromatograms, a typical example of which is shown in Figure 1, there is clear resolution of all hydrocarbons and enrichment of longer chain *n*-alkanes (LHC, C_{25} to C_{34}), compared to the shorter chain

n-alkanes (SHC, C_8 to C_{24}). The sum of hydrocarbons of the two ranges (∑LHC and ∑SHC) followed similar trend in all samples (Figure 2). Among SHC, the even carbon hydrocarbons (C_{16}, C_{18}, C_{20}, C_{22}) were more abundant compared to the odd carbon hydrocarbons (C_{15}, C_{17}, C_{19}, C_{21}), while among LHC, the odd carbon hydrocarbons (C_{27}, C_{29}, C_{31}, C_{33}, C_{35}) were more abundant compared to the even carbon hydrocarbons (C_{26}, C_{28}, C_{30}, C_{32}, C_{34}; Figure 3). The abundance of the C_{31} hydrocarbon was the highest among all hydrocarbons (Figure 3).

The carbon preference index (CPI) was calculated separately for LHC and SHC using the following equations[12,13]

$$CPI_{LHC} = (C_{25} + C_{27} + C_{29} + C_{31} + C_{33}) / (C_{26} + C_{28} + C_{30} + C_{32} + C_{34}), \qquad (1)$$

$$CPI_{SHC} = (C_{15} + C_{17} + C_{19} + C_{21} + C_{23}) / (C_{16} + C_{18} + C_{20} + C_{22} + C_{24}). \qquad (2)$$

The CPI of the LHC (CPI_{LHC}; 1.01–4.94, mean ± SD, 2.12 ± 1.18) was >1 and that of the SHC (CPI_{SHC}; 0.12–0.70, 0.43 ± 0.16) was <1. A plot of the CPI on the Christian Era (CE; Figure 4) shows a peak of CPI_{LHC} during the 35-year period from 1905 to 1940 (mean CPI: 3.65), and a peak of CPI_{SHC} immediately following this peak (CE 1940–1947).

The average carbon length of LHC (ACL_{LHC}) was calculated using the equation

$$ACL_{LHC} (C_{25} - C_{33}) = [25(nC_{25}) + 27(nC_{27}) + 29(nC_{29}) + 31(nC_{31}) + 33(nC_{33})] / [nC_{25} + nC_{27} + nC_{29} + nC_{31} + nC_{33}]. \qquad (3)$$

The ACL_{LHC} (C_{25}–C_{33}) ranged from 28.6 to 30.5 (mean ± SD: 29.31 ± 0.56). The ACL_{LHC} (C_{25}–C_{33}) showed a significant positive relationship with CPI_{LHC} (Figure 5).
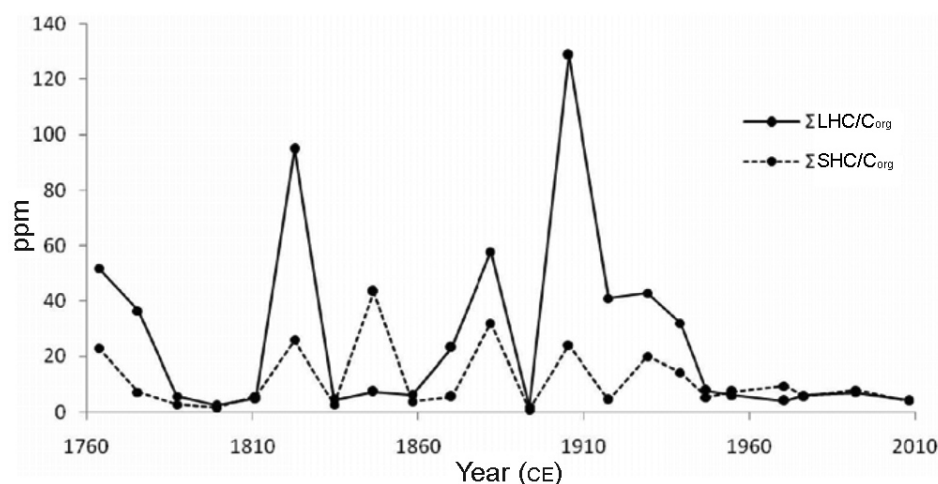
Figure 2. Sum of short-chain hydrocarbons (ΣSHC) and long-chain hydrocarbons (ΣLHC) normalized to C_{org} (the ratios of ΣLHC and ΣSHC (ppb) with C_{org} (%) were multiplied by 10 to get the unit of both ratios as ppm).
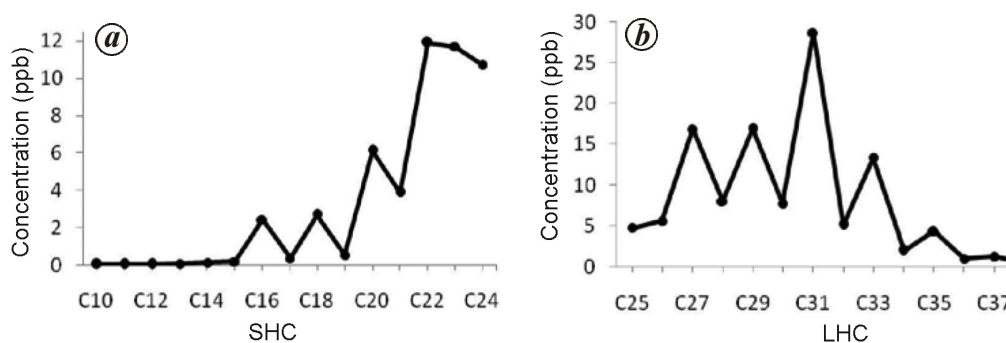

Figure 3. Average concentration (ppb) of individual hydrocarbons: *a*, SHC in which even carbon HC dominated; *b*, LHC in which odd carbon HC dominated.

The time resolution was 3.9, 7.8 and 11.7 years in the upper (0–10 cm), middle (10–20) and lower (20–65) portions of the core respectively. The THC in each of the sectional samples including surface sediment is <1 ppm, indicating that contribution by anthropogenic activity is absent[5,14,15]. As the LHC are produced by land plants and the SHC by phytoplankton, the dominance of the former (Figure 2) gives a first indication that the core sediments contain perhaps the deposits of terrestrial organic matter. But since the LHC are better preserved than the SHC in the environment[16,17], other evidences are needed to show that the stronger LHC signal is due to the dominance of terrestrial inputs.

The CPI is a commonly used tool to identify *n*-alkane sources[5,18,19]. The dominance of even carbon hydrocarbons over odd carbon hydrocarbons among the SHC, i.e. CPI < 1 (Figure 3) indeed shows that there is significant bacterial activity in the core sediments on this smaller hydrocarbon fraction[17,20]. In the LHC, the predominance of odd hydrocarbons compared to even hydrocarbons (Figure 3, CPI > 1) does support a stronger terrestrial, i.e. higher plant wax origin[13,21–23]. The peak of CPI_{LHC} during CE 1905–1940 likely corresponds to a period of strong terrestrial signal. The peak of CPI_{SHC} immediately

following this peak during CE 1940–1947, although is for a shorter duration than the time resolution (11.7 yrs), may indicate that there was a brief period of *in situ* production following the period of peak terrestrial input.

The ACL is the average carbon number per molecule in a sediment sample, usually calculated for the odd carbon LHC in order to explore links with higher plant *n*-alkanes[24]. As the ACL_{LHC} (C_{25}–C_{33}) values are approximately constant, the natural (terrestrial) source inputs may have remained unchanged with time[24]. The linear positive, significant correlation of ACL_{LHC} (C_{25}–C_{33}) and CPI_{LHC} (Figure 5) also supports this.

The terrestrial point source closest to the core location is the River Godavari discharging annually 105 km^3 (3300 m^3 s^{-1}) of water[25] and with it 756×10^9 g of suspended particles[26]. As the deposited sediments of riverine origin, should be holding clues to the fluctuations in river discharge in the past[27], we examined the potential of CPI_{LHC} as a proxy of discharge from the Godavari. The data of discharge rates of the Godavari at Polavaram for the past 100 years were collected from the Central Water Commission, Hyderabad. The discharge rates were averaged for the duration that the corresponding sectional sediments have age resolution, and plotted against CPI_{LHC}
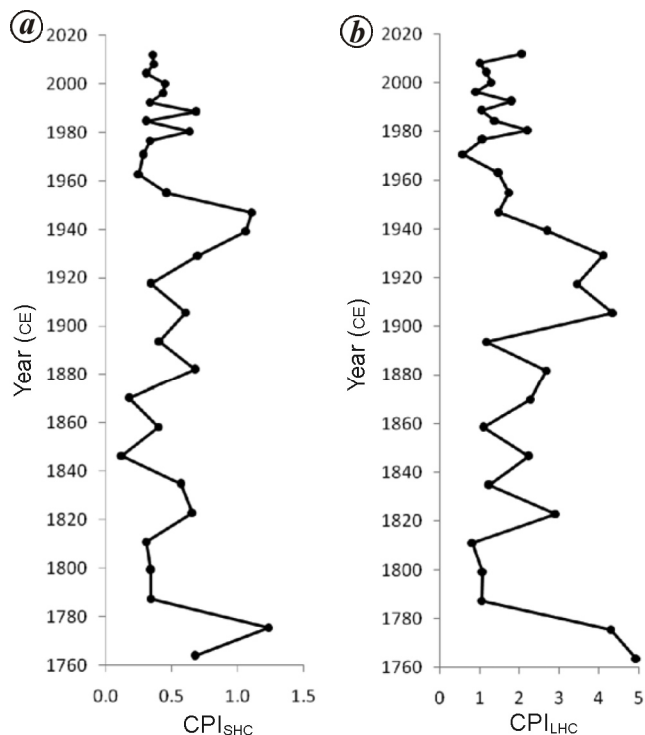
Figure 4. Profile of carbon preference index (CPI) of (*a*) SHC (CPI$_{SHC}$) and (*b*) LHC (CPI$_{LHC}$) in the sediment core (*Y*-axis: sediment depth converted to year on the Christian Era).
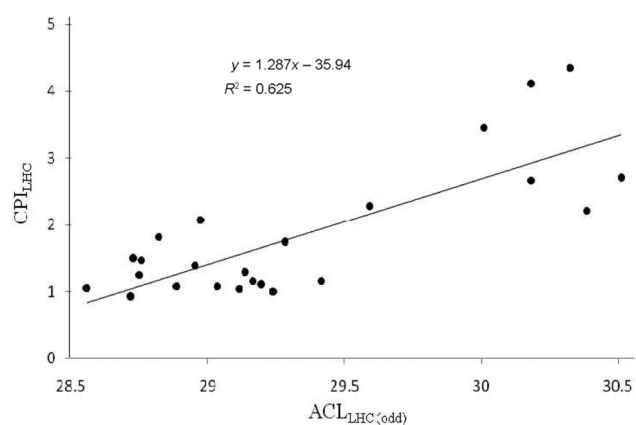

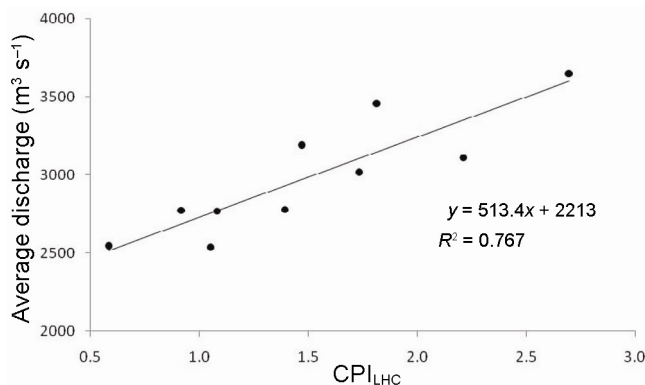**Figure 5.** Average chain length (ACL) of LHC (ACL$_{LHC}$) versus CPI$_{LHC}$.

Figure 6. Historical discharge of River Godavari versus CPI$_{LHC}$.

(Figure 6). There was highly significant linear positive correlation between the two for the period 1930–1996 ($R^2 = 0.77$, $n = 10$, $P = 0.0004$), indicating that the CPI$_{LHC}$ is a reasonably good proxy of the river discharge for that period. The correlation was somewhat lower ($R^2 = 0.51$, $P = 0.0033$) when more recent data (1997–2008) of the top sediments of the core were also included, and attributed to early diagenetic reactions.

In the sediments, the long-chain hydrocarbons ($\geq C_{25}$), which are of terrestrial origin are well preserved, unlike the short-chain hydrocarbons of marine (*in situ*) origin ($\leq C_{24}$) which were partly removed by bacterial metabolism. The significant linear relationship of the odd over even carbon preference index of longer chain hydrocarbons (CPI$_{LHC}$) with the corresponding discharge data from the Godavari may be useful to predict past changes in discharge pattern of the river, whose drainage basin constitutes over 9% area of the Indian land mass. The study has assumed a uniform sedimentation rate, although coastal processes may not allow it to be so. A higher resolution study in more cores is expected to improve the relationship between CPI$_{LHC}$ and discharge from the River Godavari.

1. Wang, X. C., Sun, S., Ma, H. Q. and Liu, Y., Sources and distribution of aliphatic and polyaromatic hydrocarbons in sediments of Jiaozhou Bay, Qingdao, China. *Mar. Pollut. Bull.*, 2006, **52**, 129–138.
2. Gogou, A., Bouloubassi, I. and Stephanou, E. G., Marine organic geochemistry of the Eastern Mediterranean: 1. Aliphatic and polyaromatic hydrocarbons in Cretan Sea surficial sediments. *Mar. Chem.*, 2000, **68**, 265–282.
3. Volkman, J. K., Marine organic matter: biomarkers, isotopes and DNA. *Life Sci. Handbook Mar. Chem.*, 2006, 2N, 2.
4. Wu, Y., Zhang, J., Cho, K. W., Hong, G. H. and Chung, C. S., Origin and transport of sedimentary organic matter in the Yalujiang Estuary, North China. *Estuaries*, 2004, **27**, 583–592.
5. Volkman, J. K., Holdsworth, D., Neill, G. and Bavor, H., Identification of natural, anthropogenic and petroleum hydrocarbons in aquatic sediments. *Sci. Total Environ.*, 1992, **112**, 203–219.
6. Brassell, S. C. and Eglinton, G., Molecular geochemical indicators in sediments. *ACS Symposium Series (Org. Mar. Geochem.)*, 1986, **305**, 10–32.
7. Rao, L. H. J., Rao, T. S., Reddy, D. R. S. and Biswas, N. R., Morphology and sedimentation of continental slope, rise and abyssal plain of western part of Bay of Bengal. *Geol. Surv. India Spec. Publ.*, 1992, **29**, 209–217.
8. El Wakeel, S. K. and Riley, J. P., The determination of organic carbon in marine muds. *J. Cons. Int. Pour l'exploration de la Mer.*, 1956, **22**, 180–183.
9. Somayajulu, B. L. K., Bhushan, R., Sarkar, A., Burr, G. S. and Jull, A. J. T., Sediment deposition rates on the continental margins of the eastern Arabian Sea using ^{210}Pb, ^{137}Cs and C. *Sci. Total Environ.*, 1999, **237/238**, 429–439.
10. Cutshall, N. H., Larsen, I. L. and Olsen, C. R., Direct analysis of Pb-210 in sediment samples: self-absorption correction. *Nucl. Instrum. Methods*, 1983, **206**, 309–312.
11. Zheng, G. J. and Richardson, B. J., Petroleum hydrocarbons and polycyclic aromatic hydrocarbons (PAHs) in Hong Kong marine sediments. *Chemosphere*, 1999, **38**(11), 2625–2632.
12. Ekpo, B. O., Fubara, P. E., Ekpa, D. O. and Marynowski, L. H., Hydrocarbon sources, n-alkanes, polycyclic aromatic hydrocarbons,

PAH distribution indices, factor analysis, Bonny river. *ARPN J. Earth Sci.*, 2012, **1**, 9–20.

13. Brassell, S. C., Eglington, G., Maxwell, J. R. and Philp, R. P., Natural background of alkanes in the aquatic environment. In *Aquatic Pollutants: Transformation and Biological Effects*, Pergamon Press, Oxford, 1978, pp. 69–86.

14. Punyu, V. R., Harji, R. R., Bhosle, N. B. and Sawant, S. S., *n*-Alkanes in surficial sediments of Visakhapatnam Harbour, east coast of India. *J. Earth Syst. Sci.*, 2013, **122**, 467–477.

15. Farrington, J. W. and Tripp, B. W., Hydrocarbons in western North Atlantic surface sediments. *Geochim. Cosmochim. Acta*, 1997, **41**, 1627–1641.

16. Ekpo, B. O., Oyo-Ita, O. and Wehner, H., Even *n*-alkane/alkene predominances in surface sediments from the Calabar River, S.E. Niger Delta, Nigeria. *Naturwissenschaften*, 2005, **92**, 341–346.

17. Elias, V. O., Simoneit, B. R. T. and Cardoso, J. N., Even *n*-alkane predominances on the Amazon Shelf and a Northeast Pacific Hydrothermal System. *Naturwissenchaften*, 1997, **84**, 415–420.

18. Hu, L., Guo, Z., Feng, J., Yang, Z. and Fang, M., Distributions and sources of bulk OM and aliphatic hydrocarbons in the surface sediments of the Bohai Sea, China. *Mar. Chem.*, 2009, **113**, 197–211.

19. Mille, G., Asia, L., Guiliano, M., Malleret, L. and Doumenq, P., Hydrocarbons in coastal sediments from the Mediterranean Sea (Gulf of Fos area, France). *Mar. Pollut. Bull.*, 2007, **54**, 566–575.

20. Grimalt, J. and Albaiges, J., Sources and occurrence of C12–C22 *n*-alkane distributions with even carbon number preference in sedimentary environments. *Geochim. Cosmochim. Acta*, 1987, **51**, 1379–1384.

21. Ahad, J. M. E., Ganeshram, R. S., Bryant, C. L., Cisneros-Dozale, L. M., Ascough, P. L., Fallick, A. E. and Slater, G. L., Sources of *n*-alkanes in an urbanized estuary: insights from molecular distributions and compound-specific stable and radiocarbon isotopes. *Mar. Chem.*, 2011, **126**, 1–4.

22. Pearson, A. and Eglinton, T. I., The origin of *n*-alkanes in Santa Monica Basin surface sediment: a model based on compound-specific δ^{14}C and δ^{13}C data. *Org. Geochem.*, 2000, **31**, 1103–1116.

23. Ishiwatari, R., Hirakawa, Y., Uzaki, M., Yamada, K. and Yada, T., Organic geochemistry of the Japan Sea sediments: 1. Bulk organic matter and hydrocarbon analyses of core KH-79-3, C-3 from the Oki Ridge for paleoenvironment assessment. *J. Oceanogr.*, 1994, **50**, 179–195.

24. Jeng, W., Higher plant *n*-alkanes average length as an indicator of petrogenic hydrocarbon contained in marine sediments. *Mar. Chem.*, 2006, **102**, 242–251.

25. Rao, K. L., *India's Water Wealth, its Assessment, Uses and Projections*, Orient Longman, New Delhi, 1975, p. 255.

26. Balakrishna, K. and Probst, J. L., Organic carbon transport and C/N ratio variations in a large tropical river: Godavari as a case study, India. *Biogeochemistry*, 2005, **73**, 457–473.

27. Tripathy, G. R., Singh, S. K., Bhushan, R. and Ramaswamy, V., 2010. Sr–Nd isotope composition of the Bay of Bengal sediments: impact of climate on erosion in the Himalaya. *Geochem. J.*, 2011, **45**, 175–186.

Polarimetric classification of C-band SAR data for forest density characterization

A. O. Varghese* and A. K. Joshi

Regional Remote Sensing Centre-Central,
National Remote Sensing Centre, Nagpur 440 001, India

Polarimetric classification is one of the most significant applications of synthetic aperture radar (SAR) remote sensing. Sensitivity of C-band SAR in discerning the variation in canopy roughness and limited penetration capability through forest canopy have been well studied at a given frequency, polarization and incidence angle. However, the scope of C-band SAR in characterizing and monitoring forest density has not been adequately understood with polarimetric techniques. The objectives of the present study were to understand the scattering behaviour of different land-cover classes and evaluate the feasibility of polarimetric SAR data classification methods in forest canopy density slicing using C-band SAR data. The RADARSAT-2 image with fine quad-pol obtained on 27 October 2011 over Madhav National Park, Madhya Pradesh, India and its surroundings was used for the analysis. Forest patches exhibit α-angle around 45°, which means the dominant scattering mechanism is volume; entropy of one or a value close to it denotes distributed targets and low anisotropy values than all other land units, which shows a dominant first scattering mechanism. This study comparatively analysed Wishart supervized classifier and Support Vector Machine (SVM) classifier for classification of the forest canopy density along with other associated land-cover classes for a better understanding of the class separability. All forest density classes showed comparatively good separability in Wishart supervized classification (73.8–84.7%) and in SVM classifier (82.3–84.8%). The results demonstrate the effectiveness of SVM classifier (88.7%) over Wishart supervized classifier (87.8%) with kappa coefficient of 0.86 and 0.85 respectively. The experimental results obtained with polarimetric C-band SAR data over dry deciduous forest area imply that SAR data have a significant potential for estimating stand density in operational forestry.

Keywords: Forest density, microwave radiation, polarimetric classification, synthetic aperture radar.

FOREST cover mapping based on species identification and forest density is an important activity for forest management and biomass estimation, which in turn is crucial for global environmental monitoring. India is among the few countries in the world to start such a unique system of monitoring of forest cover at the national level. At present, Indian forests are monitored by optical remote

---